Assessing the Performance of Solar Cells Based on MoS_2: WS_2 and WSe_2 Buffer Layers Effects

A. Aouragh[a], F. Selloum[b], S. Djeffal[b], T. Bouarroudj[c], C. Shekhar[d], S. Maamri[e] and B. Zaidi[b,*]

[a] *Department of Chemistry, Faculty of Material Sciences, University of Batna 1, Batna, Algeria*
[b] *Department of Physics, Faculty of Material Sciences, University of Batna 1, Batna, Algeria*
[c] *Scientific and technical research center in physico-chemical analyses (CRAPC), BP 384, Bou-ismail, RP 42004, Tipaza, Algeria*
[d] *Department of Applied Physics, Amity University Gurgaon, Haryana, India 122413*
[e] *Department of Applied physics, Faculty of Sciences, University of Salamanca 1, Salamanca, Spain*

Received: 09.12.2023 & Accepted: 22.02.2024

Doi: 10.12693/APhysPolA.145.242 *e-mail: beddiaf.zaidi@univ-batna.dz

In this study, we simulated the performance of solar cells using appropriate optical and electrical parameters for MoX_2 compounds. We used the solar cell capacitance simulator software to simulate MoS_2-based solar cells with two structures ($ZnO/WS_2/MoS_2$ or $ZnO/WSe_2/MoS_2$). We investigated the impact of varying the thickness of the MoS_2 absorbing layer, doping, temperature elevation, and exploring the effect of the buffer layer on the electrical characteristics of the solar cell, including parameters like open-circuit voltage (V_{oc}), short-circuit current (J_{sc}), and solar cell efficiency (η). This analysis aimed to provide valuable insights into optimizing the design and performance of MoS_2-based solar cells, contributing to advancements in thin-film solar cell technology.

topics: WS_2, WSe_2, MoS_2; solar cell; thin film; solar cell capacitance simulator (SCAPS-1D)

1. Introduction

Silicon currently serves as the predominant semiconductor in photovoltaic applications. Despite continuous technological advancements that reduce the manufacturing costs of silicon solar cells, the inherently high material costs of silicon persist [1, 2]. A potential substitute for wafer-based crystalline silicon solar cells are thin-film solar cells with polycrystalline $Cu(In,Ga)Se_2$ (CIGS) absorber layers [3–5]. These thin films represent a viable option for diversifying the photovoltaic landscape, considering that crystalline silicon cells currently dominate global installations.

Additionally, transition metal dichalcogenides thin films (TMDs), compounds characterized by a layered structure [6–12], such as MX_2 (M = W, Mo; X = Se, S, Te), play a crucial role in various technologies. These technologies include optoelectronics [13–15], field effect transistors [16, 17], and photovoltaic cells [18]. Molybdenum disulfide (MoS_2) stands out as a promising and cost-effective option for capturing sunlight, potentially serving as an alternative to conventional photovoltaic materials. Its viability as a photovoltaic absorber is underlined by its optimal optical and electrical properties, making it a compelling candidate for consideration in the quest for efficient and economical solar energy solutions [19]. The band gap of MoS_2 varies from indirect to direct, ranging between 1.2 and 1.8 eV. This variability, along with its beneficial optoelectronic properties, such as the absorption coefficient of about 2.8×10^6 cm^{-1} (with a statistical uncertainty of $\pm 1.3 \times 10^5$ cm^{-1}), has prompted the analysis of MoS_2-based solar cells in previous research [20–23] to enhance the performance of photovoltaic cell structures.

This study aims to employ SCAPS-1D simulation software to explore the effect of different parameters on photovoltaic performance. The goal is to provide a streamlined approach for predicting optimal conditions without the need for the actual fabrication and characterization of $ZnO/(WS_2$ or $WSe_2)/MoS_2$ solar cells. This methodology offers a practical means for assessing and optimizing the performance of solar cells.

2. Device modeling

To determine the effect of solar radiation on the performance of solar cells, simulation software such as AMPS, wxAMPS, PC1D, Afors-Het, ASA, SILVACO, and SCAPS-1D can be used. In this

TABLE I

Simulation parameters of MoS_2-based solar cell.

Parameter	MoS_2	WS_2	WSe_2	ZnO
thickness [μm]	0.5–1.5	0.1	0.1	0.08
band gap [eV]	1.58	2.3	1.72	3.40
electronic affinity [eV]	4.2	4.2	4.0	4.55
dielectric permittivity	13.6	13.6	13.6	10
effective state density of BC [cm^{-3}]	2.2×10^{18}	2.2×10^{18}	2.2×10^{18}	10^{18}
Effective state density of BV [cm^{-3}]	1.8×10^{19}	1.8×10^{19}	1.8×10^{19}	9×10^{19}
electron mobility [$cm^2/(V\ s)$]	100	100	100	100
hole mobility [$cm^2/(V\ s)$]	25	25	180	25

Fig. 1. Structure of a solar cell simulated using SCAPS-1D.

study, we used SCAPS-1D software to simulate the photovoltaic process of $ZnO/(WS_2$ or $WSe_2)/MoS_2$ solar cells [24–26] as shown in Fig. 1.

The solar cell capacitance simulator software (SCAPS-1D) necessitates simulation input data relating to each layer involved in the design of the solar cell, which are summarized in Table I. Parameters for ZnO, WS_2, WSe_2, and MoS_2 were derived from prior theoretical simulations papers [10, 27–29]. The thermal velocities of electrons and holes in each layer were approximated at 10^7 cm/s for simplicity in numerical analysis. Molybdenum (Mo) and aluminum (Al) serve as rear and front contacts.

3. Results and discussion

Figures 2, 3, and 4 illustrate, respectively, the variation of the short circuit current (J_{sc}), open circuit voltage (V_{oc}), and the efficiency (η) as a function of the thickness of the absorbent layer MoS_2. We changed the thickness of the MoS_2 absorbing layer in the range from 0.5 to 1.5 μm. An increase in efficiency, short-circuit current, and open circuit voltage of the solar cell is observed with the increase in the thickness of the MoS_2 absorbing layer. From a comparative analysis between the two cells, we see that the cell with the WSe_2 buffer layer is better than the cell with the WS_2 buffer layer.

This work enables us to determine the optimal MoS_2 absorbing layer thickness of 1.5 μm, optimizing the operational characteristics of our solar cell structure.

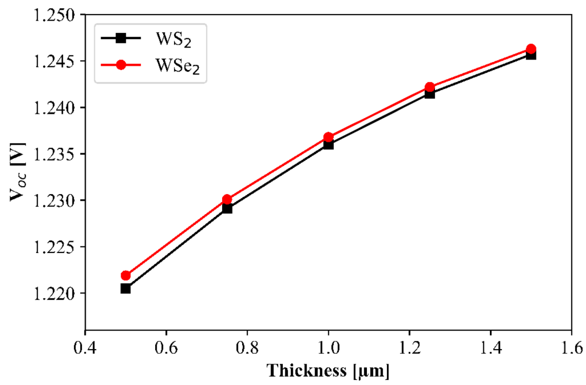

Fig. 2. MoS_2 absorbing layer thickness effect on the open circuit voltage (V_{oc}).

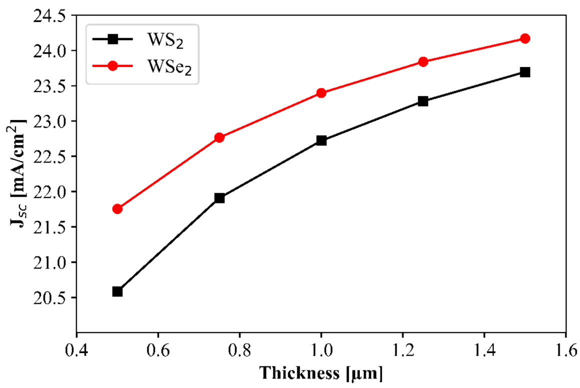

Fig. 3. MoS_2 absorbing layer thickness effect on the short-circuit current (J_{sc}).

Figures 5, 6, and 7 depict, respectively, the open circuit voltage (V_{oc}), the short circuit current (J_{sc}), and the efficiency (η) with respect to solar cell temperature. From the results shown in Figs. 5–7, we note that the efficiency and the open circuit voltage decrease with the increase in environmental temperature, and the short circuit current increases with the increase in environmental temperature. It is concluded that the cell with the WSe_2 buffer layer gives better results at high temperatures compared to the cell with the WS_2 buffer layer. Solar

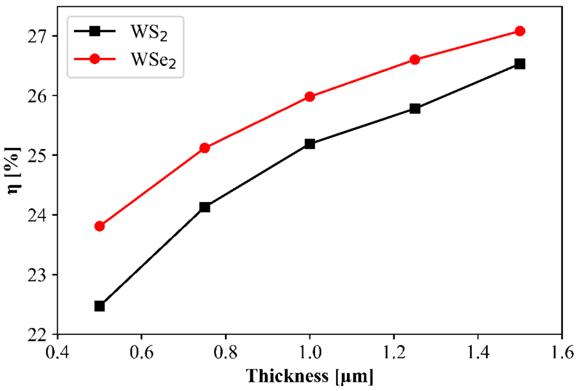

Fig. 4. MoS_2 absorbing layer thickness effect on solar cell efficiency (η).

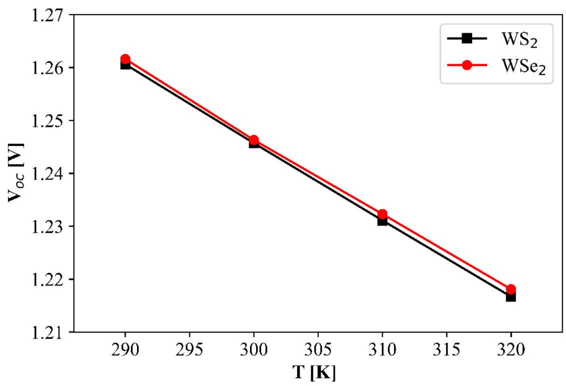

Fig. 5. Open circuit voltage (V_{oc}) variation vs solar cell temperature.

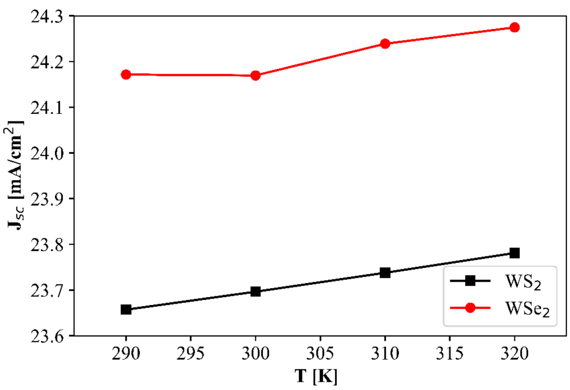

Fig. 6. Short-circuit current (J_{sc}) variation vs solar cell temperature.

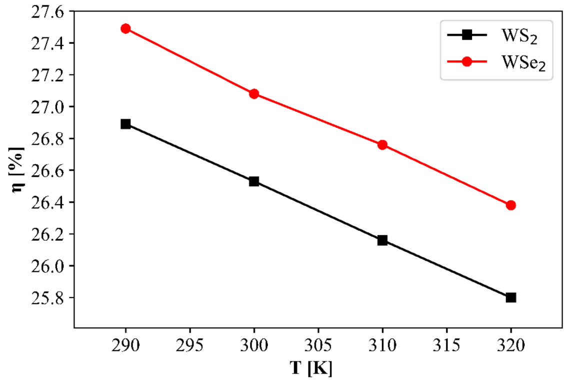

Fig. 7. Efficiency (η) variation vs solar cell temperature.

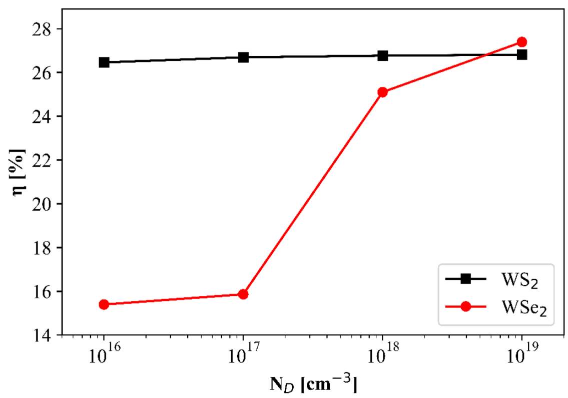

Fig. 8. Influence of donor concentration N_D on solar cell efficiency (η).

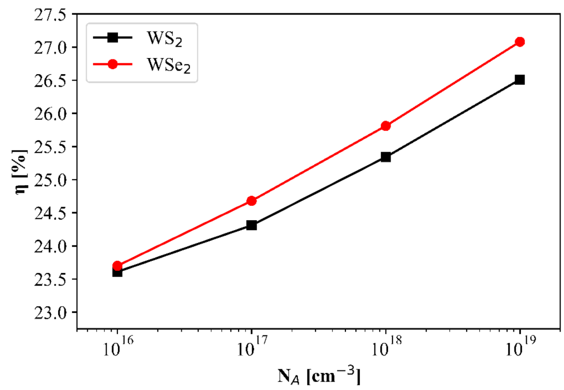

Fig. 9. Effect of concentration of acceptors N_A in the MoS_2 layer on the efficiency (η).

panels that exhibit reduced temperature sensitivity are preferable in hot regions, while those with higher temperature responsiveness prove more effective in colder climates [30].

In order to study the influence of doping of the WS_2 or WSe_2 buffer layer, we varied the concentration of the N_D donors from 10^{16} to 10^{19} cm^{-3}, as shown in Fig. 8. We observed that the efficiency increases with the density of N_D donor carriers. It is observed that the efficiency (η) of the solar cell with the WSe_2 buffer layer increases significantly, while the efficiency of the solar cell with the WS_2 buffer layer increases very little.

Figure 9 shows the effect of varying the doping of the absorbent layer on the efficiency (η). It is observed that the efficiency decreases when the doping of the MoS_2 layer is increased. It is found that the solar cell with the WSe_2 buffer layer is affected

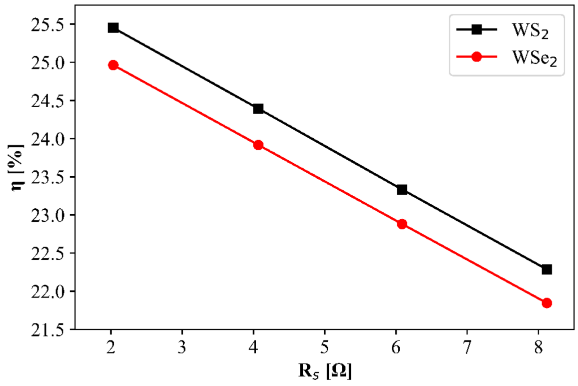

Fig. 10. Influence of series resistance on the efficiency (η) of ZnO/(WS_2 or WSe_2)/MoS_2.

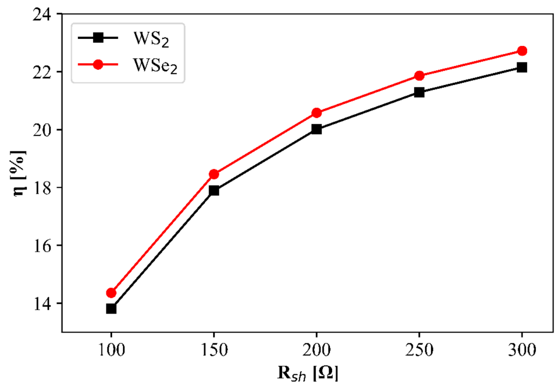

Fig. 11. Effect of shunt resistance on efficiency (η) of ZnO/(WS_2 or WSe_2)/MoS_2.

by a higher donor concentration than the solar cell with the WS_2 buffer layer. The findings have been reported in scientific literature [31].

According to Fig. 10, we see that the increase in series resistance from 2 to 8 Ω led to a reduction in efficiency (η). The increase in the value of the series resistance of ZnO/(WS_2 or WSe_2)/MoS_2 has been found to cause a decrease in the efficiency. The efficiency drops significantly from 25.5 to 21.8%. The results are presented in scientific literature [32].

Figure 11 shows the variation in efficiency (η) of ZnO/(WS_2 or WSe_2)/MoS_2 as a function of shunt resistance. We observe that the increase in shunt resistance leads to an increase in efficiency. The performance increases by 13.9% to 23% as the value of the shunt resistance is increased from 100 to 300 Ω. Several authors [33, 34] in the literature have reported similar results.

4. Conclusions

In this paper, we studied the effect of certain parameters on the electrical properties of solar cells based on MoS_2 with different buffer layers (WSe_2 or WS_2) using the SCAPS-1D software. The simulation results that we obtained clearly show that the open circuit voltage (V_{oc}), short circuit current (J_{sc}), and efficiency (η) increase with increasing thickness of the MoS_2 absorber layer. The results proved a negative correlation between temperature and photovoltaic parameters such as efficiency and open circuit voltage. Conversely, the correlation between temperature and short circuit current increases with the rise of environmental temperature. The buffer layer plays a very important role in the solar cell structure, because when replacing the WS_2 buffer layer with the WSe_2 buffer layer, we noticed an improvement in the electrical characteristics of the solar cell. The efficiency increases with higher concentrations of donors and acceptors in the MoS_2 absorbing layer. The rise in the series resistance of ZnO/(WS_2 or WSe_2)/MoS_2 has been observed to lead to a reduction in efficiency. The efficiency increases when the shunt resistance increases and vice versa for the shunt resistance.

Acknowledgments

The authors would like to extend their sincere gratitude to Marc Burgelman and his team at Ghent University for providing access to SCAPS-1D.

References

[1] R. Barrio, N. Gonzalez, J. Cárabe, J.J. Gandía, *JOM* **72**, 608 (2020).

[2] O. Martinez, J. Mass, A. Tejero, B. Moralejo, V. Hortelano, M. González, J. Jiménez, V. Parra, *Acta Phys. Pol. A* **125**, 1013 (2014).

[3] T.D. Lee, A.U. Ebong, *Renew. Sustain. Energy Rev.* **70**, 1286 (2017).

[4] B. Zaidi, M. Zouagri, S. Merad, C. Shekhar, B. Hadjoudja, B. Chouial, *Acta Phys. Pol. A* **136**, 988 (2019).

[5] R. Prasad, R. Pal, U.P. Singh, *Superlattices Microstruct.* **161**, 107094 (2022).

[6] B. Zaidi, C. Shekhar, B. Hadjoudja, S. Gagui, B. Chouial, *Acta Phys. Pol. A* **136**, 495 (2019).

[7] K.S. Novoselov, A. Mishchenko, A. Carvalho, A.H. Castro Neto, *Science* **353**, aac9439 (2016).

[8] L. Zheng, X. Wang, H. Jiang, M. Xu, W. Huang, Z. Liu, *Nano Res.* **15**, 5781 (2022).

[9] Y. Lv, P. Chen, J.J. Foo, J. Zhang, W. Qian, C. Chen, W.J. Ong, *Mater. Today Nano* **18**, 100191 (2022).

[10] B. Zaidi, C. Shekhar, B. Hadjoudja, S. Gagui, M.A. Saeed, *Trans. Electr. Electron. Mater.* **22**, 687 (2021).

[11] X. Yuan, B. Zhou, X. Zhang, Y. Li, L. Liu, *Electrochim. Acta* **283**, 1163 (2018).

[12] Y.J. Park, H.S. So, H. Hwang, D.S. Jeong, H.J. Lee, J. Lim, C.G. Kim, H.S. Shin, *ACS Nano* **16**, 11059 (2022).

[13] K.F. Mak, J. Shan, *Nat. Nanotechnol.* **17**, 686 (2022).

[14] S. Tongay, J. Zhou, C. Ataca, K. Lo, T.S. Matthews, J. Li, J.C. Grossman, J. Wu, *Nano Lett.* **12**, 5576 (2012).

[15] P. Walke, R. Kaupmees, M. Grossberg-Kuusk, J. Krustok, *ACS Omega* **8**, 37958 (2023).

[16] J. Chang, L.F. Register, S.K. Banerjee, *J. Appl. Phys.* **115**, 084506 (2014).

[17] S. Larentis, B. Fallahazad, E. Tutuc, *Appl. Phys. Lett.* **101**, 223104 (2012).

[18] M. Bernardi, M. Palummo, J.C. Grossman, *Nano Lett.* **13**, 3664 (2013).

[19] H. Rashid, K.S. Rahman, M.I. Hossain, N. Tabet, F.H. Alharbi, N. Amin, *Chalcogenide Lett.* **11**, 397 (2014).

[20] A.-J. Cho, M.-K. Song, D.-W. Kang, J.-Y. Kwon, *ACS Appl. Mater. Interfaces* **10**, 35972 (2018).

[21] J.D. Yao, G.W. Yang, *Nano Today* **36**, 101026 (2021).

[22] M.H. Ali, M.A. Al Mamun, M.D. Haque, M.F. Rahman, M.K. Hossain, A.Z.M. Touhidul Islam, *ACS Omega* **8**, 7017 (2023).

[23] Y. Jiang, S. Chen, W. Zheng, B. Zheng, A. Pan, *Light Sci. Appl.* **10**, 72 (2021).

[24] K. Decock, S. Khelif, M. Burgelman, *Thin Solid Films* **519**, 7481 (2011).

[25] M. Burgelman, J. Verschraegen, S. Degrave, P. Nollet, *Prog. Photovolt. Res. Appl.* **12**, 143 (2004).

[26] M. Burgelman, P. Nollet, S. Degrave, *Thin Solid Films* **361–362**, 527 (2000).

[27] R. Mahbub, M.S. Islam, F. Anwar, S.S. Satter, S.M. Ullah, *South Asian J. Eng. Technol.* **2**, 1 (2016).

[28] P.K. Dakua, D.K. Panda, *Phys. Scr.* **98**, 085402 (2023).

[29] S. Gohri, J. Madan, R. Pandey, R. Sharma, in: *2021 IEEE 48th Photovoltaic Specialists Conf. (PVSC), Fort Lauderdale (FL)*, 2021, p. 2020.

[30] S. Dubey, J. N. Sarvaiya, B. Seshadri, *Energy Procedia* **33**, 311 (2013).

[31] D. Vikraman, A.A. Arbab, S. Hussain, N.K. Shrestha, S.H. Jeong, J. Jung, S.A. Patil, H.S. Kim, *ACS Sustain. Chem. Eng.* **7**, 13195 (2019).

[32] J. Ding, X. Cheng, T. Fu, *Vacuum* **77**, 163 (2005).

[33] E. Radziemska, *Energy Conv. Manag.* **46**, 1485 (2005).

[34] P. Singh, S.N. Singh, M. Lal, M. Husain, *Solar Energy Mater. Solar Cells* **92**, 1611 (2008).